Int. J. Electrochem. Sci., 16 **(2021)** Article Number: 211216, doi: 10.20964/2021.12.51

International Journal of
ELECTROCHEMICAL
SCIENCE
www.electrochemsci.org

MoO_2 nanoparticles anchored on hierarchical carbon architectures for fast K-ion storage

Liming Chen[1], *Bin Huang*[1,*], *Jianwen Yang*[1], *Yanwei Li*[1], *Quanqi Chen*[1], *Shunhua Xiao*[1], *Wei Li*[1,2,*]

[1] Guangxi Key Laboratory of Electrochemical and Magneto-chemical Functional Materials, College of Chemistry and Bioengineering, Guilin University of Technology, Guilin 541004, China.
[2] College of Environmental Science and Engineering, Guilin University of Technology, Guilin 541004, China.
[*]E-mail: bin@glut.edu.cn

Received: 23 August 2021 / *Accepted:* 9 October 2021 / *Published:* 10 November 2021

Monodisperse spherical architectures consisting of MoO_2 nanoparticles and polydopamine-derived carbon matrices are designed and successfully synthesized. X-ray diffraction revealed that the MoO_2 nanoparticles are crystalline state whereas the carbon matrices are amorphous. The hierarchical morphology is confirmed by scanning electron microscope and transmission electron microscope. Electrochemical characterizations demonstrate that the composite can achieve fast K-ion storage, which enable its potential application in K-ion batteries. For optimizing the synthesis condition, different calcination temperatures are adopted. The sample synthesized at 500 ^{o}C exhibits the highest capacity in K-ion storage, as well as the best rate capability. Furthermore, study on the kinetics of electrode process reveals that the unique architecture shows significant capacitive behavior, verifying the fast K-ion storage capability.

Keywords: Energy storage and conversion; Nanocomposites; Molybdenum oxide; hierarchical; potassium-ion batteries

1. INTRODUCTION

Lithium-ion batteries (LIBs) have achieved great success in various applications ranging from consumer electronics and wireless tools to electric vehicles. Nevertheless, the limited nature of lithium mineral reserves hinders the infinite expansion of the manufacture of LIBs[1]. Hence, adequate alternatives should be developed. Among the electrochemical energy storage systems, sodium-ion batteries (SIBs) and potassium-ion batteries (PIBs) have attracted considerable attentions due to the abundant sodium and potassium mineral reserves, as well as the similar electrochemical behaviors to LIBs[2-4]. Unfortunately, the lithium storage materials are unable to be directly transplanted into SIBs

and PIBs; moreover, the existing electrode materials for Na-/K-ion storages perform much worse than those for Li-ion storage caused by the larger radii of Na^+ and K^+, especially for the K-ion storage materials, making them unable to satisfy commercial applications[5].

Recently, great effort has been devoted to exploiting transition metal oxides (TMOs) for K-ion storage due to their high theoretical capacity and rich sources of raw materials. Among TMOs, MoO_2 (and its derivatives) is considered as a promising material due to its high specific capacity and, more importantly, much higher electrical conductivity than other TMOs (~190 S cm^{-1})[6,7]. However, TMOs suffer from significant volume variations during charge/discharge cycles since their reversible energy storages are dominated by conversion mechanisms[8]. Many strategies have been proposed to suppress the drawback and improve the electrochemical performance, including reducing particle size to nanoscale[9], constructing heterojunctions with other compounds[10], combining active materials with robust and highly-conductive matrices (*e.g*. graphene, hard carbon, etc.)[11], and so on.

Herein we introduce a spherical hierarchical architectures consisting of MoO_2 nanoparticles and polydopamine-derived carbon matrices as a promising anode material for PIBs. This composite exhibits high reversible specific capacity and cyclic stability. Besides, outstanding long-term cycle life is achieved at high current density. The effect of synthesis temperature on the electrochemical performance is also studied.

2. EXPERIMENTAL

For preparation of MoO_2/C composite, first of all, 4 g of $(NH_4)_6Mo_7O_{24}\cdot 4H_2O$ and 1 g of dopamine hydrochloride were dissolved in 400 mL of distilled water with stirring. Then 800 mL of ethanol was poured into the aforementioned solution with vigorous stirring to form a dark orange solution, followed by adding 6 mL $NH_3\cdot H_2O$. After stirring for 2 h, the orange Mo-polydopamine precipitate was harvested by centrifugation, washed with ethanol and distilled water for several times and dried at 70 ^oC overnight. Finally, the samples were obtained by calcining the Mo-polydopamine at 350 ^oC, 500 ^oC and 700 ^oC under Ar flow for 2 h.

The crystallographic structure of the as-prepared sample was determined by X-ray diffraction (XRD) using a PANalytical X'Pert Pro X-ray diffractometer. The morphology was observed using scanning electron microscope (SEM, FEI Helios Nanolab 600i) and transmission electron microscope (TEM, FEI Tecnai G2 F-20, 200 kV).

CR 2016 coin-type cells were assembled with fresh-made potassium pieces as counter electrodes for electrochemical studies. Electrodes were composed of 80 wt% as-prepared sample, 10 wt% Super P carbon black and 10 wt% sodium carboxymethyl cellulose (CMC-Na) binder. 1 M KPF_6 in 1:1 vol% EC/DEC was used as electrolyte. The cells were assembled in an Ar-filled glove box (Braun) with O_2 and H_2O lower than 0.5 ppm.

3. RESULTS AND DISCUSSION

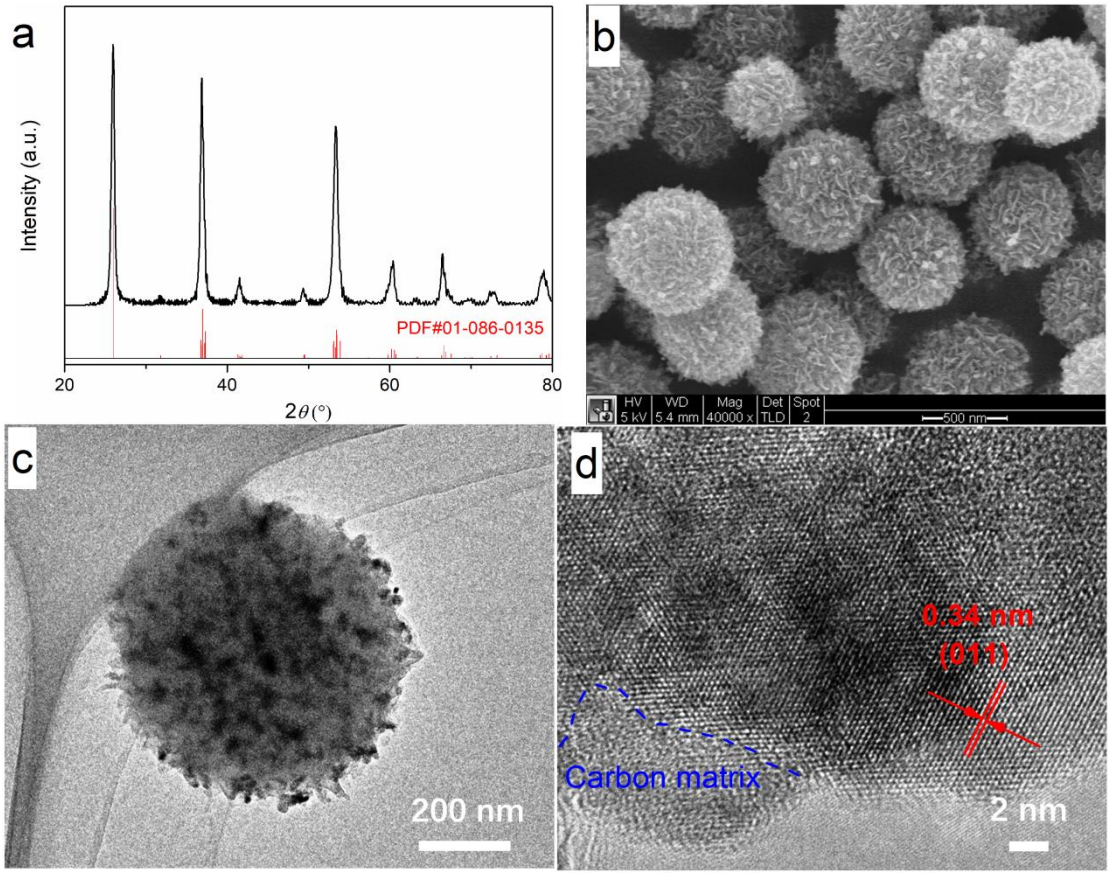

Figure 1. XRD pattern (a), SEM image (b) and TEM images (c, d) of the MoO_2/C synthesized at 500 ^oC.

The results of crystallographic and microscopic analyses on the sample synthesized at 500 ^oC are shown in Fig. 1. The peaks in Fig. 1a can be indexed to MoO_2 (Tugarinovite, PDF# 01-086-0135). Crystalline carbon cannot be identified through this pattern, suggesting that the carbon matrix is amorphous. Fig. 1b shows the SEM image of the sample, in which monodisperse spherical architectures with an average diameter of 500 nm can be seen. Obviously one spherical architecture is composed of numerous nanoplates, thus can be considered as a hierarchical structure. Detailed microstructure can be observed from the TEM and high-resolution TEM (HRTEM) results, as shown in Fig. 1c and d. It can be clearly seen from Fig. 1c that the hierarchical sphere is composed of MoO_2 nanoparticles (dark discrete dots) and carbon matrix (gray). From Fig. 1d the lattice fringes with a spacing of 0.34 nm, corresponding to the (011) facet of MoO_2, together with the amorphous region (carbon matrix), can be observed.

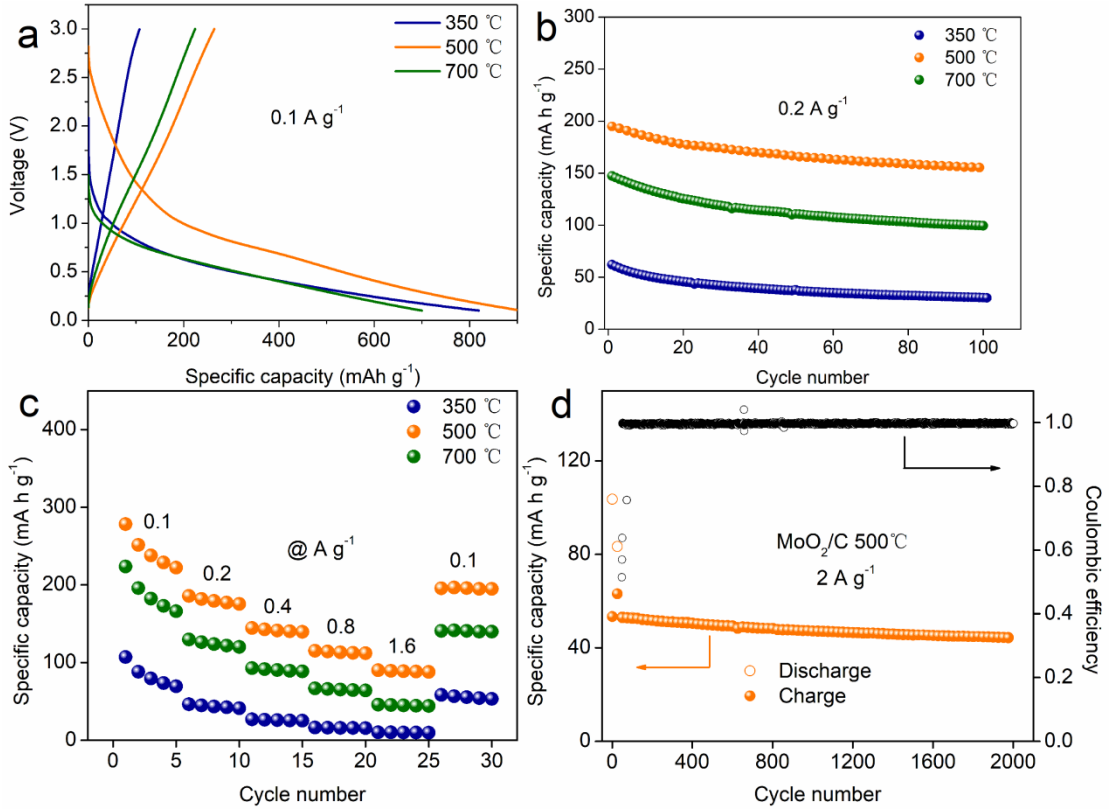

Figure 2. Comparison of initial charge-discharge plots (a), cycling performance (b) and rate capability (c) of the samples synthesized at different temperatures, together with the long-term cycling performance of the MoO_2/C synthesized at 500 ^oC (d).

Fig. 2 shows the electrochemical properties of the as-prepared samples. For comparison, the data collected from the ones synthesized at different temperatures is plotted together. As can be seen in Fig. 2a, the initial charge-discharge curves were measured at a current density of 0.1 A g^{-1}. The sample synthesized at 500 ^oC delivers the highest reversible capacity of 264.1 mAh g^{-1}. The ones calcined at 350 ^oC and 700 ^oC exhibit initial capacities of 107.2 and 223.7 mAh g^{-1}, respectively. All the samples show remarkable capacity loss in the first cycle, which is mainly attributed to the solid-electrolyte interphase (SEI) formation. Fig. 2b shows the cycling performance at a current density of 0.2 A g^{-1} of the three samples. Only charge (de-potassiation) capacities are plotted. Before cycling, all the samples underwent three charge-discharge cycles at 0.1 A g^{-1} for activation. It can be seen that the sample synthesized at 500 ^oC has the highest capacity; after 100 cycles it shows a residual capacity of 155.2 mA g^{-1}, with a capacity retention of 79.6%. By contrast, the ones calcined at 350 and 700 ^oC only deliver 30.3 and 99.5 mAh g^{-1} at the 100th cycle, with the retentions of 48.8% and 67.5%, respectively. In addition, the former also presents strong ability in tolerating high current densities. As displayed in Fig. 2c, it delivers a specific capacity of ~89 mA h g^{-1} at a high current density of 1.6 A g^{-1}. In contrast, the latter two only have capacities of ~10 and ~45 mA h g^{-1} at the same current density, respectively. Hence, 500 ^oC is considered as the optimum temperature for the synthesis of MoO_2/C in our experiment. To test the long-term cycling performance, the sample synthesized at 500 ^oC was cycled at

2 A g^{-1} for 2000 cycles. As shown in Fig. 2d, a reversible capacity of ~47 mAh g^{-1} remains after 2000 cycles.

It demonstrated that K ions prefer to adsorb on the surface of MoO_2 rather than intercalate into the structure[12]. Hence, the active material cannot be fully utilized for K-ion storage, which results in low specific capacity. An effective strategy is to design some special architectures which possess relatively high specific surface area. In this work, the hierarchical spherical architecture can provide high specific surface area for K-ion adsorption. Besides, the carbon matrix acts as a conductive network to facilitate the charge transfer. Therefore, this composite exhibits excellent electrochemical performance. For comparison, the electrochemical performances in K-ion storage for some other MoO_2-based materials are listed in Table 1. It can be seen that the as-prepared sample shows competitive performance among the similar materials reported in other works.

Table 1. Comparison of electrochemical performances between the as-prepared sample and similar materials reported

Sample	Reversible capacity (mAh g^{-1}) at low current density	Rate capability (mAh g^{-1}) / current density	Reference
MoO_2/C	264.1 at 0.1 A g^{-1}	89 at 1.6 A g^{-1}	This work
MoO_2-rGO	~ 320 at 0.1 A g^{-1}	~ 0 at 2 A g^{-1}	[12]
MoO_2/rGO	367.2 at 0.05 A g^{-1}	176.4 at 0.5 A g^{-1}	[13]
MoO_2/3DPC	344 at 0.05 A g^{-1}	~140 at 1 A g^{-1}	[14]

The charge storage behavior of the sample synthesized at 500 ºC has been further studied using cyclic voltammetry (CV). As can be seen in Fig. 3a, two broad peaks located at 0.65 and 0.26 V are observed in the first cathodic scan, associating with the formation of SEI layer and potassiation of MoO_2, respectively. In the following anodic and cathodic processes, the CV curves do not show distinct redox peaks, suggesting that significant capacitive behavior dominates the K-ion storage process. The degree of capacitive contribution can be analyzed according to the relationship between current response and scan rate[15]

$$i=av^b=k_1v+k_2v^{1/2}$$

where a and b are empirical constants that could be obtained by a logarithmic (*log*) plot of i with v (the scan rate). b = 0.5 indicates a battery-type electrochemical behavior, and b = 1.0 implies a capacitor-type process[8]. Therefore, the current response (i) at a fixed potential can be separated into capacitive (k_1v) and diffusion-controlled ($k_2v^{1/2}$) behaviors. The CV curves swept from 0.2 to 1.0 mV s^{-1} are shown in Fig. 3b, which display a similar contour. As shown in Fig. 3c, most b values of the cathodic and anodic peaks are identified between 0.6 and 1.0, indicating a capacitor-dominant contribution. By calculating the constants k_1 and k_2, we can distinguish the portions of the current from capacitive and diffusion-controlled contributions. The result, shown in Fig. 3d, reveals that the capacitive process contributes 72 % of the current response, verifying the fast kinetics in K-ion storage of the material.

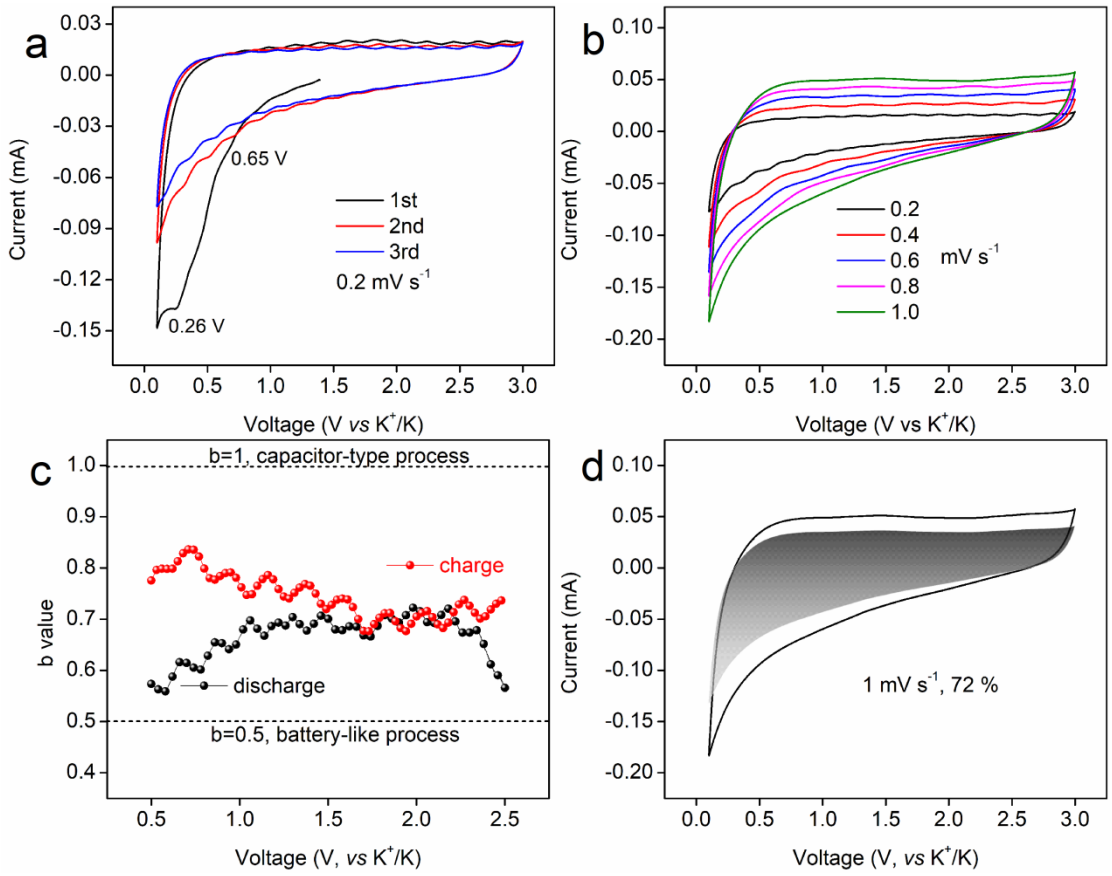

Figure 3. CV curves of the MoO_2/C (500 ºC) at (a) a scan rate of 0.2 mV s^{-1} and (b) various scan rates, together with the (c) *b* value distributions and (d) capacitive contribution in the CV curve (gray region).

4. CONCLUSIONS

In summary, monodisperse spherical architectures consisting of MoO_2 nanoparticles and polydopamine-derived carbon matrices have been synthesized and studied as an anode material for PIBs. The sample synthesized at 500 ºC exhibited the highest reversible specific capacity and cyclic stability. Besides, outstanding long-term cycle life was also achieved at a high current density of 2 A g^{-1}. It was demonstrated that the capacitive behavior could contribute a significant portion to the capacity, revealing the reason for the fast K-ion storage. This work has guidance significance to the design of molybdenum-based anode materials for PIBs.

ACKNOWLEDGEMENTS
This work was supported by the Guangxi Natural Science Foundation (2017GXNSFBA198141) and the Science and Technology Base and Talent Project of Guangxi (GUIKEAD20159049).

References

1. B. Huang, J. Yang, Y. Li, S. Xiao and Q. Chen, *Mater. Lett.*, 210 (2018) 321.

2. X. Zhao, W. Cai, Y. Yang, X. Song, Z. Neale, H. E. Wang, J. Sui and G. Cao, *Nano Energy*, 47 (2018) 224.
3. I. Sultana, M. M. Rahman, Y. Chen and A. M. Glushenkov, *Adv. Funct. Mater*., 28 (2018) 1703857.
4. Y. Li, Q. Zhang, Y. Yuan, H. Liu, C. Yang, Z. Lin and J. Lu, *Adv. Energy Mater*., 10 (2020) 2000717.
5. B. Huang, Z. Pan, X. Su and L. An, *J. Power Sources*, 395 (2018) 41.
6. M. Li, Y. Y. Zhu, X. Ji and S. Cheng, *Mater. Lett*., 254 (2019) 332.
7. Y. C. Rao, S. Yu, X. Gu and X. M. Duan, *Appl. Surf. Sci*., 479 (2019) 64.
8. C. T. Zhao, C. Yu, M. D. Zhang, H. W. Huang, S. F. Li, X. T. Han, Z. B. Liu, J. Yang, W. Xiao, J. N. Liang, X. L. Sun and J. S. Qiu, *Adv. Energy Mater*., 7 (2017) 8.
9. S. Bao, S. H. Luo, S. X. Yan, Z. Y. Wang, Q. Wang, J. Feng, Y. L. Wang and T. F. Yi, *Electrochim. Acta*, 307 (2019) 29.
10. Q. Jiang, S. Hu, L. Wang, Z. Huang, H. J. Yang, X. Han, Y. Li, C. Lv, Y. S. He, T. Zhou and J. Hu, *Appl. Surf. Sci*., 505 (2020) 144573.
11. Y. T. Liu, Y. Y. Xiao, F. S. Liu, P. Y. Han and G. H. Qin, *J. Mater. Chem*. A, 7 (2019) 26818.
12. J. Sheng, T. Wang, J. Tan, W. Lv, L. Qiu, Q. Zhang, G. Zhou and H.-M. Cheng, *ACS Nano*, 14 (2020) 14026.
13. C. Liu, S. Luo, H. Huang, Y. Zhai and Z. Wang, *ChemSusChem*, 12 (2019) 873.
14. S. Bao, S.-h. Luo, S.-x. Yan, Z.-y. Wang, Q. Wang, J. Feng, Y.-l. Wang and T.-f. Yi, *Electrochim. Acta*, 307 (2019) 293.
15. C. X. Hou, J. Wang, W. Du, J. C. Wang, Y. Du, C. T. Liu, J. X. Zhang, H. Hou, F. Dang, L. L. Zhao and Z. H. Guo, *J. Mater. Chem*. A, 7 (2019) 13460.